Research Article (Non-Member))

Osteochondral repair using an acellular dermal matrix – Pilot *in Vivo* study in a rabbit osteochondral defect model[1]

Ken Ye, PhD[1,2], *Kathy Traianedes 0000-0003-2279-481X, PhD[3,4], Shalley A. Robins, BSc (Hons)[4], Peter F.M. Choong, MD[1,2] and Damian E. Myers, PhD[4,5,6] .

[1] Department of Surgery, St Vincent's Hospital Melbourne, University of Melbourne, Fitzroy, Australia

[2] Department of Orthopaedics, St Vincent's Hospital Melbourne, Fitzroy, Australia

[3] Department of Clinical Neurosciences, St Vincent's Hospital Melbourne, Fitzroy, Australia,

[4] Department of Medicine, St Vincent's Hospital and Western Health, University of Melbourne, Fitzroy, Australia

[5] Victoria University, Sunshine Hospital, St Albans, Australia

[6]Australian Institute for Musculoskeletal Science, Victoria University and The University of Melbourne, Western Centre for Health and Research Education, Sunshine Hospital, St Albans, Australia

All studies were performed at St Vincent's Hospital Melbourne, Fitzroy, Australia

* Author for correspondence

Dr. Kathy Traianedes

Address: Department Clinical Neurosciences

St Vincent's Hospital, Melbourne

Victoria Parade, Fitzroy 3065

Tel.: +61 3 9231 3526

[1] This is the author manuscript accepted for publication and has undergone full peer review but has not been through the copyediting, typesetting, pagination and proofreading process, which may lead to differences between this version and the Version of Record. Please cite this article as doi:10.1002/jor.23837

Fax: +61 3 9231 3350

Email: kathy.traianedes@svha.org.au

Running title: Osteochondral repair with biological matrix

Keywords: Cartilage, Osteochondral, Acellular dermal matrix, Tissue engineering, Stem Cells

Author contribution: KY and KT contributed to experimental design, data acquisition, review and analysis, manuscript preparation and revision; SR contributed to *in vitro* rabbit data; DEM contributed to experimental design, data review, and manuscript preparation and revision; PMC contributed to critical review of the manuscript

Author statement: All authors have read and approved the final submitted manuscript.

Abstract

The aim of this pilot project was to introduce a novel use of acellular dermal matrix (ADM) in combination with infrapatellar fat pad mesenchymal stromal cells (IPFP-MSCs) to effect repair in a rabbit osteochondral defect model. ADM, in a range of surgical procedures, has been shown to promote remodelling of tissue at the site of implantation. Rabbit-derived ADM (rabADM) was prepared from the skin of donor rabbits. Autologous IPFP-MSCs were obtained at the time of knee surgery. Osteochondral defects (4mm cartilage outer/2mm central bone defect) were drilled into distal femoral condyles of 12 New Zealand White rabbits. Treatments groups: (1) Defect only, (2) rabADM alone, (3) IPFP-MSCs alone, and (4) rabADM with IPFP-MSCs. Condyles were harvested at 12 weeks, and analyzed using histology, immunohistochemistry (type I and II collagen) and histomorphometry to evaluate osteochondral repair. The rabADM only group achieved the highest ratio of type II to non-type II collagen (77.3%) using areal measures (equivalent to normal cartilage), which indicated a higher quality of cartilage repair. The addition of IPFP-MSCs, with or without rabADM, formed a fibrous collagen cap above the lesion site not seen with rabADM alone. Macroscopically, there was no joint erosion, inflammation, swelling or deformity, and all animals maintained full range of motion. Conclusions: RabADM alone resulted in neocartilage formation similar to native cartilage. IPFP-MSCs limited osteochondral repair and contributed to fibrosis, even in combination with the rabADM. Further studies using ADM for osteochondral repair are warranted in a more appropriate pre-clinical model of osteochondral repair.

Background

Osteochondral repair has been difficult due to the lack of intrinsic capacity for cartilage to regenerate [1, 2]. Fibrocartilage that normally forms in response to cartilage damage is not normal tissue and lacks the compressive and hydrodynamic qualities of normal hyaline

cartilage, and eventually leads to cartilage and bone degradation causing joint dysfunction and pain [3].

Approaches to osteochondral repair include debridement, marrow stimulation via microfracture, osteochondral grafting, and autologous chondrocyte implantation (ACI) [4-6]. Some procedures provide symptomatic relief without changing the natural course of degenerative disease [7, 8]. Microfracture usually results in formation of fibrocartilage [9, 10]. Although some studies reported good early results, these eventually deteriorate [11, 12]. Similarly, osteochondral grafting [13], ACI [14, 15], and matrix-induced autologous chondrocyte implantation (MACI) [16] have shown some improvements over microfracture, but long-term results are variable [17]. An approach that will achieve good long-term clinical outcomes is needed.

Current tissue engineering approaches to cartilage repair include the use of biocompatible scaffolds with cells. Acellular biological scaffolds, comprising of extracellular matrix (ECM) components maintained in their natural state that can aid cellular repopulation, differentiation, and proliferation, has been utilized in tissue repair [18] and may hold a key for improved articular cartilage regeneration. Many scaffolds (single and multiple components) are available for clinical use [18], however there is a minimal data available of long-term outcomes with these products. Although cross-linked acellular cartilage matrices have been described for repair of chondral and osteochondral defects, [19-21] translation to the clinic is problematic. A meta-analysis on the utility of acellular biomaterials for cartilage repair of an osteochondral defect concluded that the presence of acellular biomaterials was better than empty defect [22].

Acellular dermal matrix (ADM), originally described by Livesey *et al*. (1995) [23], is prepared using a unique decellularization process, which preserves ECM structure and biochemistry, does not illicit an inflammatory or tissue rejection response following allogeneic

transplantation, and the transplanted graft exhibits revascularization and host cell repopulation [23]. The human equivalent, AlloDerm®, has since been used in diverse clinical surgical applications including abdominal wall reconstruction [24], alloplastic breast reconstruction [25], and vaginal repair [26]. These reports highlight and reinforce the ability of the ADM to remodel to tissue at the site of implantation. The natural architectural complexity of the ECM is maintained in the ADM compared to the single component biomaterials [22]. Several sources of cells have been trialed for cartilage repair applications. The infrapatellar fat pad (IPFP) may contain immunoactive cells [27] that may mediate pro- and/or anti-inflammatory responses. IPFPs are also a source of mesenchymal stem cells, similar to pluripotent bone marrow-derived stem cells [28, 29] with similar proliferative and chondrogenic differentiation capacities [30, 31].

The hypothesis of this study is that a natural intact ADM, alone or in combination with IPFP-MSCs, can promote osteochondral repair. The aim of this study was to determine whether rabbit-derived ADM, alone or in combination with autologous IPFP-MSCs, can repair an osteochondral defect in the rabbit femoral condyle in a one-step, single-site surgical procedure. This short-term pilot study was used to screen the efficacy of the acellular scaffold with and without inclusion of local stromal cells as a prelude to conducting the treatment in a more relevant pre-clinical model of osteochondral repair.

Methods

Animal ethics

Animal experiments were approved by St Vincent's Hospital Melbourne (SVHM) Animal Ethics Committee (AEC). All animal studies were conducted in accordance with the Australian Code for the Care and Use of Animals for Scientific Purposes (8th Edition). Animals were obtained from Nanowie Small Animal Production Unit (Modewarre, Victoria, Australia) or S&J Hurrell (Cowra, NSW, Australia) and maintained at SVHM.

Rabbit acellular dermal matrix processing

Full-thickness skin was harvested from three neonatal New Zealand White (NZW) rabbits (gender irrelevant) for preparation of rabbit-derived ADM (rabADM). The rabbit skin was cut to obtain a dermal thickness of approximately 250-300μm thickness (Figure 1A) (rabbit knee cartilage thickness) using a Leica VT1000 Vibratome (Leica Microsystems, Wetzlar, Germany) to isolate the epidermis/dermis prior to decellularisation (achieved by gluing the skin (Scotch-Weld cyanoacrylate (3M Corp. St Paul, MN, USA)), hair-side down, onto adhesive tape on the Vibratome platform). The blade was elevated approximately 1mm from the surface of the platform to achieve a cut through the dermis. The tape-adhered tissue (now containing the epidermis/dermis) was subsequently processed. During the initial steps of epidermis removal(using several non-denaturing detergent steps), the epidermis (along with the hair) (Figure 1A) remained adhered to the tape and was separated from the dermis (white tissue) and discarded. Decellularization was achieved using the original method [23, 32] and U.S. Patents 5,336,616 and 4,865,871. Briefly, the aseptic process involves removal of the epidermis (Figure 1A), followed by removal of dermal cells and cyroprotection in a carbohydrate complex solution. The cyroprotected rabADM was then packed in sterile poly-Tyvek pouches (Beacon Converters Inc. Saddle Brook, NJ, USA), sealed and freeze-dried (Virtis Genesis 25L freeze-dryer, SP Industries Warminster, PA, USA). The freeze-dried tissue was subsequently packed and sealed under nitrogen atmosphere in foil pouches (Beacon Converters Inc.) and stored at -80°C until use. Removal of cells negates the potential for a specific immune response. Maintaining the structural integrity (cryopreservation and freeze-drying) of the matrix removes any potential non-specific inflammatory response following transplantation. RabADM was characterized histologically and compared to fresh tissue (rabADM). Previous experiments have demonstrated that the decellularization and freeze-drying process do not result in collagen degradation, and collagen banding patterns are

identical between fresh and processed dermis (results not shown), as described by Livesey et al. [23]. *In vitro* microbiological assessment was performed for anaerobic and aerobic bacteria detection over 14 days of culture (all negative; results not shown). *In vivo* biocompatibility testing of the processed rabADM was performed by subdermal implant in immune-competent NZW rabbits (21 days, n=3 animals) to identify any potential graft issues (e.g. sterility or graft damage). Routine haematoxylin and eosin (H&E) staining was performed on paraffin-embedded explants (Figure 1C). Explants were assessed histologically for evidence of fibrous encapsulation, inflammatory responses (including extrusion, edema, and purulent formation) and biological responses (revascularization (Figure 1D and E), host integration, and cellular repopulation).

***In vitro* chondrogenic potential of rabbit IPFP-MSCs**

Rabbit IPFP-MSCs were isolated from three adult NZ white rabbits as described below. The *in vitro* chondrogenic potential of rabbit IPFP-MSCs was demonstrated using pellet culture technique of isolated cells treated under the same chondrogenic conditions (in the presence of the growth factors TGF-β3 and BMP-6) as previously described for human IPFP cells [32-34] (Figure 2). Resulting pellets were stained with H&E, toluidine blue and expression of type I and II collagen were detected by immunohistochemistry as described below.

Rabbit osteochondral model

Osteochondral defects were created in the weight-bearing aspect in the femoral condyles of both hind limbs of 12 young adult female NZW rabbits (acclimated weight 2.8±0.2kg, mean±SD) after subcutaneous injection of pre-anesthetic and general anesthesia (Ketamine 35mg/kg (CEVA Animal Health Pty Ltd, Glenorie, NSW, Australia) and Xylazine 5mg/kg (Troy Laboratories Pty Ltd, Glendenning, NSW, Australia)). Animals were maintained under Isoflurane (AbbVie Pty Ltd, Botany, NSW, Australia)/oxygen for the duration of the procedure. Animals received analgesic of Carprofen 1.5mg/kg (Carprofen Ventral™, Sigma-

Aldrich Corp., St Louis, MO, USA) subcutaneously post-surgery. Once anaesthetized, the rabbits' knees and groin were shaved and skin decontaminated using 70% alcoholic chlorhexidine solution (Biotech Pharmaceuticals Pty Ltd, Laverton North, Victoria, Australia). A midline longitudinal incision was made over the knee joint followed by a medial parapatellar approach to the knee. A limited quadriceps release was required to mobilize the patella, which was then dislocated laterally. IPFPs were removed from rabbit knees with a scalpel and placed in sterile saline then diced using fine scissors prior to collagenase digestion. The knee was flexed to reveal the weight bearing areas of the femoral condyles. A 4mm stainless steel drill bit (Sutton, NZ) was used to create a chondral defect in the center of the femoral medial condyle. This was followed by the drilling of a 2mm hole using a stainless steel drill bit (Sutton, NZ) in the center of the 4mm defect to penetrate into the subchondral bone (at a depth of approximately 2mm), thus creating an osteochondral defect (see Figure 3A and 3C (schematic)).

Animals were randomly allocated to the treatment groups (the same treatment was not consecutively performed). For the rabADM groups, freeze-dried rabADM was brought to room temperature and rehydrated in sterile normal saline (Baxter International Inc., Deerfield, IL, USA). Two and 4mm diameter discs of rabADM were created using sterile skin biopsy punches (Kai Medical, Solingen, Germany): 2mm rabADM was used to fill the 2mm defect and Tisseel fibrin sealant (Baxter) was used to fix the 4mm rabADM in the defect site according to manufacturer instructions (see Figure 3B).

Subsequently, the patellar was relocated and the surgical site was closed using 4-0 Monocryl sutures (Ethicon, Johnson & Johnson Medical, Somerville, NJ, USA). The skin was closed with a subcuticular continuous stitch (5-0 Monocryl suture) (Ethicon) and reinforced with interrupted sutures where necessary. All operated knees were immobilized using a plaster cast for seven days at approximately 90°-100° of flexion. Animals were allowed to recover

on a heat pad before being returned to their pen. Animals were monitored by animal technicians daily. Once the plaster was removed, the rabbits were allowed to mobilize freely in open pens (hay bedding) for the remainder of the 12 weeks. Access to food and drink was *ad libitum.* Rabbits were humanely killed using inhalation anesthesia followed by intra-cardiac injection of Lethobarb (Virbac Australia Pty Ltd, Milperra, NSW, Australia). The knees were harvested for histological analysis as described.

Autologous IPFP harvest and re-implantation

Harvested IPFPs were diced and tissue digested in 0.2% collagenase (types I and II) (Worthington Biochemical Corporation, Lakewood, NJ, USA) in DMEM (Lonza Group, Basel, Switzerland) supplemented with antibiotics (Gibco, Life Technologies, Carlsbad, CA, USA) for one hour at 37°C under constant agitation, as previously described [33, 34]. The digest was filtered through a 40µm filter (BD Falcon, Bedford, MA, USA) and washed three times, followed by re-suspension of the cell pellet in sterile phosphate buffered saline (PBS) (Gibco) before the cells were counted (Scepter™, Merck Millipore, Billerica, MA, USA). Approximately 90,000 (89,500±17,564 cells) were inserted into each defect (within the subchondral region, through the 2mm central drill hole). The defect sites with cells were left uncovered or covered using 2 and 4mm plugs of rabADM (as shown in Figure 3).
The four treatment groups were: (1) defect only, (2) rabADM only, (3) IPFP-MSCs only, and (4) rabADM plus IPFP-MSCs.

Histology and immunohistochemistry

Explanted femurs were trimmed to the level of the condyles, which were then bisected along the trochlear groove using a Buehler™ IsoMet low speed bone-cutting saw (Buehler Ltd, Lake Bluff, IL, USA). Each condyle was fixed in 10% NBF (Sigma-Aldrich) for five days under vacuum, decalcified using 10% (w/v) EDTA (Sigma-Aldrich) (pH 7.2) in PBS (Gibco) for three weeks under constant agitation, and then processed for paraffin embedding. Sections

(5µm) (MICROM H325 Rotary Microtome, MICROM Interational GmbH, Waldorf, Germany) were taken at the mid-point of the defect and were stained with H&E and safranin-O/Fast green FCF (Sigma-Aldrich) [34].

Immunohistochemical assessment of type I and II collagen: Briefly, sections were pre-treated with 0.3% hydrogen peroxide (Merck Millipore, Darmstadt, Germany), subjected to Proteinase K antigen retrieval (Dako, Glostrup, Denmark) and blocked using 10% normal rabbit serum (Dako) for 30 minutes at room temperature. The primary antibodies used were: mouse monoclonal anti-human type II collagen antibody (1:500) (MP Biomedical, Solon, OH, USA); goat polyclonal anti-human type I collagen (1:500) (SouthernBiotech, Birmingham, AL, USA); and mouse monoclonal anti-human cartilage proteoglycan antibody (1:500) (Merck Millipore) for 60 minutes at 37°C. Isotype controls included goat IgG (SouthernBiotech) and mouse IgG (Invitrogen, Thermo Fisher Scientific). Secondary antibodies used were biotinylated rabbit anti-goat and rabbit anti-mouse antibodies (Dako). Secondary antibodies were applied for 30 minutes at room temperature followed by horseradish peroxidase-conjugated streptavidin using the Vectastain ABC kit according to the manufacturer's instructions (Vector Laboratories Burlingame, CA, USA). The reaction was developed using peroxidase substrate 3,3-diaminobenzidine (DAB) (Dako) for five minutes. Sections were counterstained with haematoxylin and mounted with Pertex (Histolab Products AB, Gothenburg, Sweden). Type I and II collagens were assessed by conventional techniques as reported previously [33, 34]. Other matrix components were not assessed in this study.

Histomorphometric analysis

Quality of the repair was assessed by two-dimensional areal analysis type II versus type I collagen as a percentage of the total area of cartilage repair. This measurement was performed using the CellSense Imaging software version 1.4 (Olympus, Tokyo, Japan). An example of this image analysis is shown in Figure 4.

Data analysis

Data was analyzed using GraphPad Prism 6.0 (GraphPad Software, La Jolla, CA, USA). Results are presented as the mean and standard deviation (SD) and unpaired one-way ANOVA analysis with multiple comparisons using Tukey's method were used for statistical analysis. The ROUT method to exclude outliers from all data was used with a Q value of 0.5%.

Results

Animals

Biocompatibility assessment: RabADM samples displayed no evidence of inflammation, edema, or fibrous encapsulation. All test grafts were revascularised (Figures 1D and E) and repopulated with host cells and integrated into the site (Figure 1C). *In vitro* batch testing for microbial growth was negative (results not shown). Grafts were deemed safe for knee surgeries.

Knee surgeries: All rabbits recovered well and were active after plaster removal without signs of discomfort or autophagy for the entire study. One case of wound irritation by the plaster resolved spontaneously without complication. Two rabbits were excluded from the study due to non-graft-related complications (one developed pneumonia at 10 weeks and died acutely; one developed a patellar subluxation and fusion). The remaining rabbits had no evidence of infection, inflammation, cyst formation or pain. The study number was therefore n=5 (defect sites) for each group. All rabbits gained weight throughout the study (2.8±0.2kg to 3.8±0.3kg, mean±SD). All external surgical wounds healed, joints were not deformed and had full range of motion.

Macroscopic evaluation of explanted knee joints

Images of each explanted knee are shown in Figure 5 and, qualitatively, the surrounding cartilage did not show any signs of inflammation, damage or erosion. There was some variability in the macroscopic appearance of repair within each group, from excellent macroscopic repair displaying the same color, consistency, and smoothness as the surrounding cartilage, to clear differences between the defect site and the surrounding cartilage (Figure 5). The 'cells only' and 'rabADM plus cells' groups displayed hypertrophy in the defect where the resultant tissue was raised above the joint surface by approximately 1-2 mm (Figure 5O and 5O-2). The surface of the repair in the 'defect only' group and repairs that involved the use of only cells appeared to be rougher, and the resulting tissue appeared opaque/white compared to the surrounding cartilage. In some cases, the 'defect only' group still displayed the obvious defect. There appeared to be loss of the 4mm rabADM cap from one animal (Figure 4H). The resulting analysis showed this to be an outlier in the data set and was excluded from analysis. The rabADM only group therefore was n= 4 animals).

Histology and immunohistochemistry

RabADM only group: Histological evaluation of the 'rabADM only' group, showed cartilaginous tissue which comprised mostly of type II collagen with a small proportion of type I collagen (representative image in Figure 6). Safranin-O staining was present only in the cartilage layer of the repair and a clear demarcation between cartilage and bone had formed with reformation of the tidemark (Figure 6). Chondrocyte clustering was apparent in most repairs and, some had formed columns of lacunae. The vertical integration of the rabADM with the underlying subchondral bone was excellent, which indicated the ability of this matrix to reform the correct anatomical positioning of both bone and cartilage. RabADM does not contain type II collagen, hence, the repaired tissue that contained type II collagen was produced *de novo* indicating that the correct cells had repopulated the matrix and

remodeled the matrix. Lateral integration of the rabADM was variable (from excellent lateral integration to minimal integration) but all had surrounding healthy cartilage.

Cell only group: Histological evaluation of the 'cells-only' group, showed good coverage of the defect site in most cases (representative image in Figure 6). The repair was comprised of a combination of type I and type II collagen. The base of the cartilage repair layer contained predominantly type II collagen but in most cases a fibrous cap comprised of type I collagen had formed, consistent with the macroscopic images (shown in Figure 5O and O-2). The repair appeared hypertrophic and incongruent with the surrounding tissue. Some repairs failed to regenerate subchondral bone within the centre of the repair, instead filling the hole with what appears to be fibrous tissue, which is not normal tissue (data not shown). Safranin-O staining was seen throughout the repair localizing with areas that also stained for type II collagen. Lateral integration with the surrounding cartilage was inconsistent. Vertical integration was good with formation of the tidemark in most cases.

RabADM plus cells group: The 'rabADM plus cells' group showed good defect fill (Figure 6) with regeneration of both a cartilage layer, subchondral bone and reformation of the tidemark, in most cases. Most repairs in this group consisted of a superficial fibrous layer consisting of predominantly type I collagen overlaying a deeper layer positive for type II collagen (Figure 6). This superficial fibrous layer was not seen in the rabADM alone group (Figure 6). In some cases, hypertrophic repair was noted, (Figure 5R-T) similar to that observed in the 'cell-only' group (Figure 5O). Subchondral bone formation was mostly adequate; however, in two animals, the central portion of the repair showed fibrous tissue formation. This was in contrast to the 'rabADM only' group, which did not show any fibrous tissue within the defect below the tidemark. This may indicate that, *in vivo*, these cells behave independently of the matrix and indeed interfere or compete with endogenous repair initiated by the rabADM.

Control group: The defect-only group showed either poor defect fill or some evidence of auto-repair in the lesion (Figure 6). The repair tissue showed mixed staining for type I and II collagen, typical of fibrocartilage. The partial auto-repair capability in a subchondral defect in the rabbit is well documented and is a limitation in this model, as is the size of the defect that can be created.

Histomorphometric analysis – ratio of type II to non-type II collagen: Results of the image analysis using the areal ratio of type II collagen versus non-type II collagen by conventional immunohistochemistry for quality of repair tissue are shown in Figure 7. The results of the 'rabADM group' were not significantly different to normal cartilage values (for both types II and I collagen). All other groups were significantly different to normal cartilage (i.e. significantly lower for type II collagen and significantly higher for non-type II collagen), and were similar to control (empty) group. The mean percentage of type II collagen staining in the repair tissue for the rabADM group (77.3%) was significantly greater than all other groups except for the rabADM plus cells group (57.3%). Normal cartilage was 97.0% type II collagen. Figure 7 is a graphical representation of the proportion of hyaline (type II collagen) versus fibrous tissue (non-type II collagen) within each group.

Discussion

This study demonstrated that ADM, a specially prepared acellular biological matrix, can revascularize, initiate cartilage repair in the host site, and remodel to cartilage and bone, reconstructing the correct anatomical interface of bone and cartilage. The resulting *de novo* cartilage tissue in the osteochondral defect appeared morphologically similar to normal cartilage with respect to the proportion of type II and non-type II collagen proteins present (type I collagen being the major component). Using the proportion of type II collagen to non-type II collagen proteins, the 'rabADM alone' performed better than the IPFP-MSCs alone in this osteochondral defect model. The addition of IPFP-MSCs resulted in the formation of a

superficial hypertrophic fibrous cap over the defect site, whether in the absence or presence of rabADM, promoting increased type I collagen expression. Although the rabADM plus cells group was not significantly different from 'rabADM alone' with respect to the proportions of type II collagen and I present, the 'rabADM plus cells' group was also not significantly different to the empty defect control, but was significantly different to normal cartilage. Although the *in vitro* chondrogenic potential of these cells was demonstrated (Figure 2), cell viability *in vivo* was not addressed in the current study and cell death may have contributed to the hypertrophy. Fluorescence activated cell sorting and collection of the IPFP cells displaying exclusive "stem cell" phenotype was not performed in this study as cells would require additional culturing to recover following enzyme digestion.

Scaffold-alone treatments for cartilage repair are gaining popularity [(35)]. This biological matrix supports the host's intrinsic regenerative capabilities. Integration likely occurs via revascularization, correct cell repopulation for the tissue of interest, and remodeling most likely via retention and integrity of crucial biological matrix components which may be required for stem cell recruitment/migration [(36, 37)].

Image analysis of immunohistochemistry provided key information regarding the quality and quantity extent of defect repair. Type II collagen expression is considered a marker of chondrocytic activity [(38, 39)]. The proportion of type II collagen was considered a surrogate marker for hyaline cartilage, and therefore a marker for the quality of the repair. RabADM substantially improved production of type II collagen protein, measured by immunohistochemistry and compared using area ratio of type II collagen/non-type II collagen [(40, 41)]. Results in the rabADM group reflected those measured in normal cartilage tissue. It was clear that the rabADM group performed well, and produced repairs that were mostly hyaline-like cartilage. RabADM contains no type II collagen. Therefore, the type II collagen that was produced in the defect site was generated by host cell repopulation. The ADM

provided a permissive matrix to enable true tissue regeneration, by revascularizing with host cells (to aid in ADM integration with host tissue [42, 43], before remodeling to an avascular cartilage tissue [44]... In the current study, introduction of IPFP-MSCs appears to interfere with tissue regenerative responses seen with rabADM alone resulting in generation of more fibrous-like tissue. Both these approaches (i.e. ADM alone or with cells) may induce tissue regeneration; however, the addition of extrinsic cells led to fibrosis whereas the cells recruited to the acellular dermal matrix did not.

Joint surface congruency is important in providing smooth movement at the articular surfaces. The rabADM group again provided the closest approximation to the anatomical joint surface in the resultant repaired tissue. As described above, addition of cells resulted in hypertrophy of the repair with a formation of a fibrous cap at the site. The control group typically resulted in a deficit and poor cartilage repair. Neither of these latter two outcomes is ideal.

This project used a one-step surgical procedure to achieve all elements of repair including autologous stromal cell harvest and re-implantation. Similar stem cell harvesting techniques have already been trialed in a number of studies [16, 45]. Although the results of the IPFP-MSCs in this study were considered inferior to the rabADM material alone, further uses for the IPFP-MSCs have not been discounted. For example, pre-treatment of the cells, and their efficacy in other larger animal models over longer periods of time have not been assessed.

A number of limitations were identified in this study. The major limitation was the use of a rabbit animal model. This model has a propensity towards auto repair, if the defect is of a ‘non-critical’ size. Anatomically and biomechanically, porcine or sheep models are recommended for future studies. The thin rabbit cartilage made graft fixation very difficult. Fibrin sealant may have caused some variability in the repair response, however, fibrin sealant alone has been shown to be ineffective as a treatment [46, 47]. Although fibrin has

shown some effects on cell proliferation *in vitro* [48], this does not necessarily translate *in vivo*. In fact, The ADM only group, despite having fibrin sealant present, did not form a fibrous, hypertrophic cap in any animal. The fibrin sealant may have had some impact on survival of injected cells. However, the fibrous cap also occurred in the "cells-only group" that did not have the fibrin sealant applied. The conclusion was that the fibrous cap was attributed to the cell component of the treatment. Suturing of rabADM to adjacent cartilage was considered, but other pilot studies showed that this compromised integrity of the adjacent cartilage (data not shown). Despite inherent limitations, this small animal model was appropriate for screening efficacy of scaffolds/cells for consideration in larger, more clinically relevant models such as sheep, goat and horse [49, 50].

In summary, the rabADM scaffold was biocompatible and facilitated production of hyaline-like cartilage, without hypertrophy. Restoration of the correct anatomical positioning of cartilage and bone demonstrates the plasticity of ADM with appropriate remodeling into both tissue types within the surgical site. This plasticity is demonstrated by the appearance of type II collagen in the repaired tissue not detected in rabADM before implantation. Addition of IPFP-MSCs appeared to be detrimental to repair causing consistent hypertrophy within the defect and some fibrosis within the bone region of the repair. This study has demonstrated the potential of ADM for osteochondral repair.

Acknowledgements

This work was funded through the Australian Orthopaedics Association Research Foundation and National Health and Medical Research Council Postgraduate Scholarship for author Ye (Grant number APP1017633). We acknowledge Lew Carty Foundation for the Leica Vibratome, The Eirene Lucas Foundation for the Scepter cell counter, and Lions Club

Australia and Lions Club International for the Olympus DotSlide microscope. We acknowledge Dr. Stephen Livesey's expert knowledge regarding the ADM material.

References

1. Tuan, R. S. (2007) A second-generation autologous chondrocyte implantation approach to the treatment of focal articular cartilage defects, *Arthritis Res Ther 9*, 109.
2. Vinatier, C., Bouffi, C., Merceron, C., Gordeladze, J., Brondello, J. M., Jorgensen, C., Weiss, P., Guicheux, J., and Noel, D. (2009) Cartilage tissue engineering: towards a biomaterial-assisted mesenchymal stem cell therapy, *Curr Stem Cell Res Ther 4*, 318-329.
3. Kheir, E. S. D. (2009) Management of Articular Cartilage Defects, *Orthopaedics and Trauma 23*, 266-273.
4. Knutsen, G., Drogset, J. O., Engebretsen, L., Grontvedt, T., Isaksen, V., Ludvigsen, T. C., Roberts, S., Solheim, E., Strand, T., and Johansen, O. (2007) A randomized trial comparing autologous chondrocyte implantation with microfracture. Findings at five years, *J Bone Joint Surg Am 89*, 2105-2112.
5. Bentley, G., Biant, L. C., Carrington, R. W., Akmal, M., Goldberg, A., Williams, A. M., Skinner, J. A., and Pringle, J. (2003) A prospective, randomised comparison of autologous chondrocyte implantation versus mosaicplasty for osteochondral defects in the knee, *The Journal of bone and joint surgery. British volume 85*, 223-230.
6. Saris, D. B., Vanlauwe, J., Victor, J., Haspl, M., Bohnsack, M., Fortems, Y., Vandekerckhove, B., Almqvist, K. F., Claes, T., Handelberg, F., Lagae, K., van der Bauwhede, J., Vandenneucker, H., Yang, K. G., Jelic, M., Verdonk, R., Veulemans, N., Bellemans, J., and Luyten, F. P. (2008) Characterized chondrocyte implantation results in better structural repair when treating symptomatic cartilage defects of the

knee in a randomized controlled trial versus microfracture, *The American journal of sports medicine 36*, 235-246.

7. Hubbard, M. J. (1996) Articular debridement versus washout for degeneration of the medial femoral condyle. A five-year study, *The Journal of bone and joint surgery. British volume 78*, 217-219.

8. Moseley, J. B., O'Malley, K., Petersen, N. J., Menke, T. J., Brody, B. A., Kuykendall, D. H., Hollingsworth, J. C., Ashton, C. M., and Wray, N. P. (2002) A controlled trial of arthroscopic surgery for osteoarthritis of the knee, *N Engl J Med 347*, 81-88.

9. Bae, D. K., Yoon, K. H., and Song, S. J. (2006) Cartilage healing after microfracture in osteoarthritic knees, *Arthroscopy : the journal of arthroscopic & related surgery : official publication of the Arthroscopy Association of North America and the International Arthroscopy Association 22*, 367-374.

10. Breinan, H. A., Martin, S. D., Hsu, H. P., and Spector, M. (2000) Healing of canine articular cartilage defects treated with microfracture, a type-II collagen matrix, or cultured autologous chondrocytes, *Journal of orthopaedic research : official publication of the Orthopaedic Research Society 18*, 781-789.

11. Mithoefer, K., Williams, R. J., 3rd, Warren, R. F., Potter, H. G., Spock, C. R., Jones, E. C., Wickiewicz, T. L., and Marx, R. G. (2005) The microfracture technique for the treatment of articular cartilage lesions in the knee. A prospective cohort study, *J Bone Joint Surg Am 87*, 1911-1920.

12. Clair, B. L., Johnson, A. R., and Howard, T. (2009) Cartilage repair: current and emerging options in treatment, *Foot Ankle Spec 2*, 179-188.

13. Gudas, R., Gudaite, A., Pocius, A., Gudiene, A., Cekanauskas, E., Monastyreckiene, E., and Basevicius, A. (2012) Ten-year follow-up of a prospective, randomized clinical study of mosaic osteochondral autologous transplantation versus

microfracture for the treatment of osteochondral defects in the knee joint of athletes, *The American journal of sports medicine 40*, 2499-2508.

14. Peterson, L., Minas, T., Brittberg, M., Nilsson, A., Sjogren-Jansson, E., and Lindahl, A. (2000) Two- to 9-year outcome after autologous chondrocyte transplantation of the knee, *Clinical orthopaedics and related research*, 212-234.
15. Peterson, L., Vasiliadis, H. S., Brittberg, M., and Lindahl, A. (2010) Autologous chondrocyte implantation: a long-term follow-up, *The American journal of sports medicine 38*, 1117-1124.
16. Koh, Y. G., Jo, S. B., Kwon, O. R., Suh, D. S., Lee, S. W., Park, S. H., and Choi, Y. J. (2013) Mesenchymal stem cell injections improve symptoms of knee osteoarthritis, *Arthroscopy 29*, 748-755.
17. Vanlauwe, J., Saris, D. B., Victor, J., Almqvist, K. F., Bellemans, J., and Luyten, F. P. (2011) Five-year outcome of characterized chondrocyte implantation versus microfracture for symptomatic cartilage defects of the knee: early treatment matters, *Am J Sports Med 39*, 2566-2574.
18. Jeuken, R. M., Roth, A. K., Peters, R. J. R. W., van Donkelaar, C. C., Thies, J. C., van Rhijn, L. W., and Emans, P. J. (2016) Polymers in Cartilage Defect Repair of the Knee: Current Status and Future Prospects, *Polymers 8*.
19. Cheng, N. C., Estes, B. T., Young, T. H., and Guilak, F. (2011) Engineered cartilage using primary chondrocytes cultured in a porous cartilage-derived matrix, *Regen Med 6*, 81-93.
20. Yang, Z., Shi, Y., Wei, X., He, J., Yang, S., Dickson, G., Tang, J., Xiang, J., Song, C., and Li, G. (2010) Fabrication and repair of cartilage defects with a novel acellular cartilage matrix scaffold, *Tissue Eng Part C Methods 16*, 865-876.

21. Cheng, N. C., Estes, B. T., Young, T. H., and Guilak, F. (2013) Genipin-crosslinked cartilage-derived matrix as a scaffold for human adipose-derived stem cell chondrogenesis, *Tissue engineering. Part A 19*, 484-496.

22. Pot, M. W., Gonzales, V. K., Buma, P., IntHout, J., van Kuppevelt, T. H., de Vries, R. B., and Daamen, W. F. (2016) Improved cartilage regeneration by implantation of acellular biomaterials after bone marrow stimulation: a systematic review and meta-analysis of animal studies, *PeerJ 4*, e2243.

23. Livesey, S. A., Herndon, D. N., Hollyoak, M. A., Atkinson, Y. H., and Nag, A. (1995) Transplanted acellular allograft dermal matrix. Potential as a template for the reconstruction of viable dermis, *Transplantation 60*, 1-9.

24. Buinewicz, B., and Rosen, B. (2004) Acellular cadaveric dermis (AlloDerm): a new alternative for abdominal hernia repair, *Annals of plastic surgery 52*, 188-194.

25. Breuing, K. H., and Warren, S. M. (2005) Immediate bilateral breast reconstruction with implants and inferolateral AlloDerm slings, *Annals of plastic surgery 55*, 232-239.

26. Clemons, J. L., Myers, D. L., Aguilar, V. C., and Arya, L. A. (2003) Vaginal paravaginal repair with an AlloDerm graft, *Am J Obstet Gynecol 189*, 1612-1618; discussion 1618-1619.

27. Caspar-Bauguil, S., Cousin, B., Galinier, A., Segafredo, C., Nibbelink, M., Andre, M., Casteilla, L., and Penicaud, L. (2005) Adipose tissues as an ancestral immune organ: site-specific change in obesity, *FEBS Lett 579*, 3487-3492.

28. Wickham, M. Q., Erickson, G. R., Gimble, J. M., Vail, T. P., and Guilak, F. (2003) Multipotent stromal cells derived from the infrapatellar fat pad of the knee, *Clinical orthopaedics and related research*, 196-212.

29. Dragoo, J. L., Samimi, B., Zhu, M., Hame, S. L., Thomas, B. J., Lieberman, J. R., Hedrick, M. H., and Benhaim, P. (2003) Tissue-engineered cartilage and bone using stem cells from human infrapatellar fat pads, *The Journal of bone and joint surgery. British volume 85*, 740-747.

30. Alegre-Aguaron, E., Desportes, P., Garcia-Alvarez, F., Castiella, T., Larrad, L., and Martinez-Lorenzo, M. J. (2012) Differences in surface marker expression and chondrogenic potential among various tissue-derived mesenchymal cells from elderly patients with osteoarthritis, *Cells Tissues Organs 196*, 231-240.

31. English, A., Jones, E. A., Corscadden, D., Henshaw, K., Chapman, T., Emery, P., and McGonagle, D. (2007) A comparative assessment of cartilage and joint fat pad as a potential source of cells for autologous therapy development in knee osteoarthritis, *Rheumatology (Oxford) 46*, 1676-1683.

32. Ye, K., Traianedes, K., Choong, P. F., and Myers, D. E. (2016) Chondrogenesis of Human Infrapatellar Fat Pad Stem Cells on Acellular Dermal Matrix, *Frontiers in surgery 3*, 3.

33. Felimban, R., Ye, K., Traianedes, K., Di Bella, C., Crook, J., Wallace, G. G., Quigley, A., Choong, P. F., and Myers, D. E. (2014) Differentiation of stem cells from human infrapatellar fat pad: characterization of cells undergoing chondrogenesis, *Tissue engineering. Part A 20*, 2213-2223.

34. Ye, K., Felimban, R., Traianedes, K., Moulton, S. E., Wallace, G. G., Chung, J., Quigley, A., Choong, P. F., and Myers, D. E. (2014) Chondrogenesis of infrapatellar fat pad derived adipose stem cells in 3D printed chitosan scaffold, *PloS one 9*, e99410.

35. Kon, E., Roffi, A., Filardo, G., Tesei, G., and Marcacci, M. (2015) Scaffold-based cartilage treatments: with or without cells? A systematic review of preclinical and

clinical evidence, *Arthroscopy : the journal of arthroscopic & related surgery : official publication of the Arthroscopy Association of North America and the International Arthroscopy Association 31*, 767-775.

36. Danielson, K. G., Baribault, H., Holmes, D. F., Graham, H., Kadler, K. E., and Iozzo, R. V. (1997) Targeted disruption of decorin leads to abnormal collagen fibril morphology and skin fragility, *The Journal of cell biology 136*, 729-743.

37. Young, M. F., Bi, Y., Ameye, L., and Chen, X. D. (2002) Biglycan knockout mice: new models for musculoskeletal diseases, *Glycoconj J 19*, 257-262.

38. Gudmann, N. S., Wang, J., Hoielt, S., Chen, P., Siebuhr, A. S., He, Y., Christiansen, T. G., Karsdal, M. A., and Bay-Jensen, A. C. (2014) Cartilage turnover reflected by metabolic processing of type II collagen: a novel marker of anabolic function in chondrocytes, *Int J Mol Sci 15*, 18789-18803.

39. Siebuhr, A. S., He, Y., Gudmann, N. S., Gram, A., Kjelgaard-Petersen, C. F., Qvist, P., Karsdal, M. A., and Bay-Jensen, A. C. (2014) Biomarkers of cartilage and surrounding joint tissue, *Biomark Med 8*, 713-731.

40. Meretoja, V. V., Dahlin, R. L., Wright, S., Kasper, F. K., and Mikos, A. G. (2013) The effect of hypoxia on the chondrogenic differentiation of co-cultured articular chondrocytes and mesenchymal stem cells in scaffolds, *Biomaterials 34*, 4266-4273.

41. Marlovits, S., Hombauer, M., Truppe, M., Vecsei, V., and Schlegel, W. (2004) Changes in the ratio of type-I and type-II collagen expression during monolayer culture of human chondrocytes, *J Bone Joint Surg Br 86*, 286-295.

42. Beniker, D., McQuillan, D., Livesey, S., Urban, R. M., Turner, T. M., Blum, B., Hughes, K., and Haggard, W. O. (2003) The use of acellular dermal matrix as a scaffold for periosteum replacement, *Orthopedics 26*, s591-596.

43. Menon, N. G., Rodriguez, E. D., Byrnes, C. K., Girotto, J. A., Goldberg, N. H., and Silverman, R. P. (2003) Revascularization of human acellular dermis in full-thickness abdominal wall reconstruction in the rabbit model, *Annals of plastic surgery 50*, 523-527.

44. Hallmann, R., Feinberg, R. N., Latker, C. H., Sasse, J., and Risau, W. (1987) Regression of blood vessels precedes cartilage differentiation during chick limb development, *Differentiation; research in biological diversity 34*, 98-105.

45. Lopa, S., Colombini, A., Stanco, D., de Girolamo, L., Sansone, V., and Moretti, M. (2014) Donor-matched mesenchymal stem cells from knee infrapatellar and subcutaneous adipose tissue of osteoarthritic donors display differential chondrogenic and osteogenic commitment, *Eur Cell Mater 27*, 298-311.

46. Ishii, I., Mizuta, H., Sei, A., Hirose, J., Kudo, S., and Hiraki, Y. (2007) Healing of full-thickness defects of the articular cartilage in rabbits using fibroblast growth factor-2 and a fibrin sealant, *The Journal of bone and joint surgery. British volume 89*, 693-700.

47. Kim, Y. S., Choi, Y. J., Suh, D. S., Heo, D. B., Kim, Y. I., Ryu, J. S., and Koh, Y. G. (2015) Mesenchymal stem cell implantation in osteoarthritic knees: is fibrin glue effective as a scaffold?, *The American journal of sports medicine 43*, 176-185.

48. Vavken, P., Joshi, S. M., and Murray, M. M. (2011) Fibrin concentration affects ACL fibroblast proliferation and collagen synthesis, *The Knee 18*, 42-46.

49. Frisbie, D. D., Cross, M. W., and McIlwraith, C. W. (2006) A comparative study of articular cartilage thickness in the stifle of animal species used in human pre-clinical studies compared to articular cartilage thickness in the human knee, *Vet Comp Orthop Traumatol 19*, 142-146.

50. Proffen, B. L., McElfresh, M., Fleming, B. C., and Murray, M. M. (2012) A comparative anatomical study of the human knee and six animal species, *Knee 19*, 493-499.

Figure Legends

Figure 1. Histology of rabADM – processed tissue and biocompatibility testing

The rabbit skin was cut to obtain a dermal thickness of approximately 250-300µm (Figure 1A) (average thickness of rabbit knee cartilage) using a Leica VT1000 Vibratome (Leica Microsystems, Wetzlar, Germany) to isolate the epidermis/dermis prior to decellularisation. During the initial steps of epidermis removal and decellularisation, the epidermis (along with the hair) (A) remained adhered to the tape and was separated from the dermis (white tissue) and discarded. The dermis was then processed to remove all cells as shown in (B) (H&E stained section). Biocompatibility was assessed using a 21-day subdermal implant model in normal rabbits. Explants were fixed in 10% NBF and processed for paraffin embedding. Sections of 5µm were obtained in cross-section (normal skin and implant shown) and H&E stained - the arrow depicts rabADM implant after 21 days (C). The implant showed host cell repopulation, integration into the site, and no evidence of encapsulation or inflammation. Higher magnification (black arrows to D and E), show capillaries within the graft with red cells present indicating revascularization through pre-existing channels. Scale bars as indicated.

Figure 2. Histology and immunohistochemistry of rabbit IPFP-MSCs in pellet culture at 28 days

IPFPs were harvested from rabbit knees and digested to release IPFP-MSCs which were expanded *in vitro* then pelleted (pellet cultures) and differentiated using TGF-β3 and BMP-6 to stimulate chondrogenesis. Paraffin-embedded pellets were sectioned at 5μm for H&E, toluidine blue (proteoglycans), and immunohistochemistry (type I and type II collagen) using DAB. Chondrogenic pellets showed increase chondrocytic morphology by day 28, and expressed proteoglycan, type II collagen, and some type I collagen deposition in the extracellular matrix. Control cell cultures (no chondrogenic stimuli) did not form pellets and did not exhibit chondrocytic morphology. Isotype controls are shown. Scale bars represent 500μm.

Figure 3. Rabbit condyle: defect and implantation strategy

The empty osteochondral defect is shown in (A). In the rabADM groups, 2mm diameter rabADM discs were used to fill in the central deeper 2mm hole and a 4mm diameter disc of rabADM was used to cover the entire defect, held in place with Tisseel (B). The treatment strategy is shown in (C): Defect alone (control) served as a negative control, RabADM only, IPFP-MSCs only, and rabADM plus IPFP-MSCs. In defects treated with cells, autologous IPFP-MSCs were injected into the base of the osteochondral defect and the defect was either left uncovered (cells-only group), or covered with rabADM disc (rabADM plus cells group) as indicated.

Figure 4. Quality of repair: Ratio of type II to non-type II collagen in repaired cartilage

Quality of the repair was assessed by measuring the area of type II versus non-type II collagen as a percentage of the total area of cartilage repair. The outline of the cartilage repair was traced to measure the total area of repair (green). Subsequently, the area of type II collagen staining was measured by tracing the areas stained by the type II collagen antibody (red). The non-type II collagen area includes type I collagen staining (see Figure 6). The

presence of other non-collagen matrix components was not assessed in this study. This measurement was performed using the CellSense Imaging software version 1.4 (Olympus Corporation, Hamburg, Germany).

Figure 5. Macroscopic images of explanted rabbit condyles

These are photographic images of explanted rabbit condyles: control (defect only) (A-E), rabADM only (F-J), cells only (K-O, O2), rabADM plus cells (P-T). Dotted lines mark the defect site. In all cases, there was no evidence of joint erosion or damage to surrounding cartilage. The macroscopic appearance of the repair was variable. Defect only: there were clear areas of incomplete repair where depressions remained at the defect site. RabADM only: overall showed excellent macroscopic repair, with colour, consistency and smoothness equivalent to the surrounding cartilage. Cells only: overall, the repair appeared to be rough compared to the surrounding cartilage, the repair site appeared more opaque/white compared to the surrounding cartilage; there was evidence of hypertrophy at the site with the resultant tissue being raised by 1-2mm (O-2) – see arrow). RabADM plus cells: Overall, there was good infill of tissue in the defect site. However, the site appeared similar to the 'cells only' group, with hypertrophy at the site present (T).

Figure 6. Representative histology and immunohistochemistry images

Representative H&E and safranin O (proteoglycan staining) stained images and type I and type II collagen immunohistochemistry of cartilage sections for control (empty defect), rabADM only, cells only, and rabADM plus cells groups. Sections were cut perpendicularly to the cartilage surface and sections were assessed at approximately midway through the defect site (included the 2mm central defect). Hypertrophy at the defect site is evident for the groups containing cells. Type I and II collagen expression is seen in all groups at the repair site. Variable lateral integration can be seen in all groups. The tidemark was re-established in

most cases. However, the anatomical demarcation of cartilage and bone without hypertrophy was evident in the rabADM only group.

Figure 7. Proportion of hyaline and fibrous tissue in the repair

This graph represents the proportion of type II collagen (hyaline) (black bars) and non-type II collagen tissue (hatched bars) within the repair. Normal cartilage was used as the uninjured comparison. The asterisk marks significant difference of each group when compared with normal cartilage for both type II collagen and non-type II collagen proteins. The repaired tissue in the rabADM group was predominantly type II collagen and most closely resembled normal hyaline cartilage compared with the other groups. Except for the non-significant comparisons indicated, all other groups were significantly different from the rabADM group and normal cartilage. Two-way ANOVA with multiple comparisons (Tukey's method); ***** $p<0.05$, mean ± SD; n=5 in normal cartilage, defect only, rabADM plus cells, and cells only groups; n=4 in rabADM only group (outlier excluded).

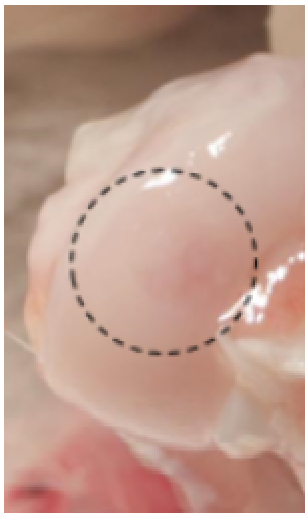

Abstract figure .

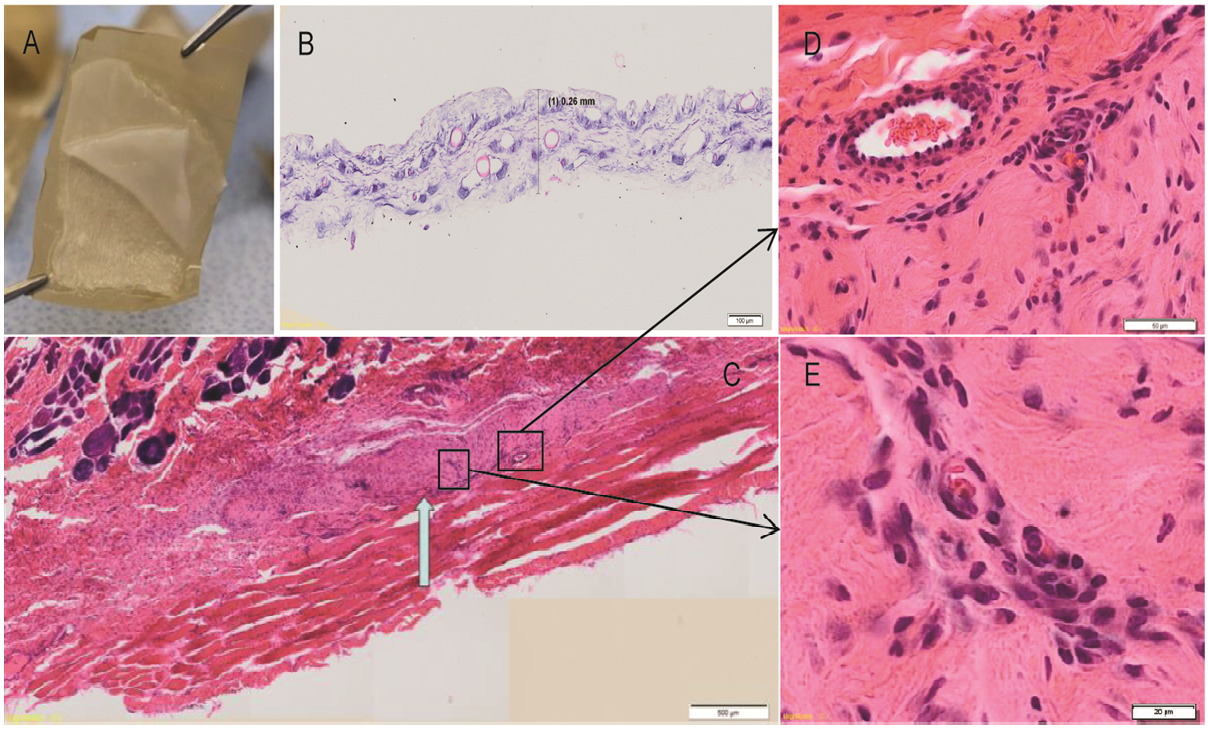

Figure 1 .

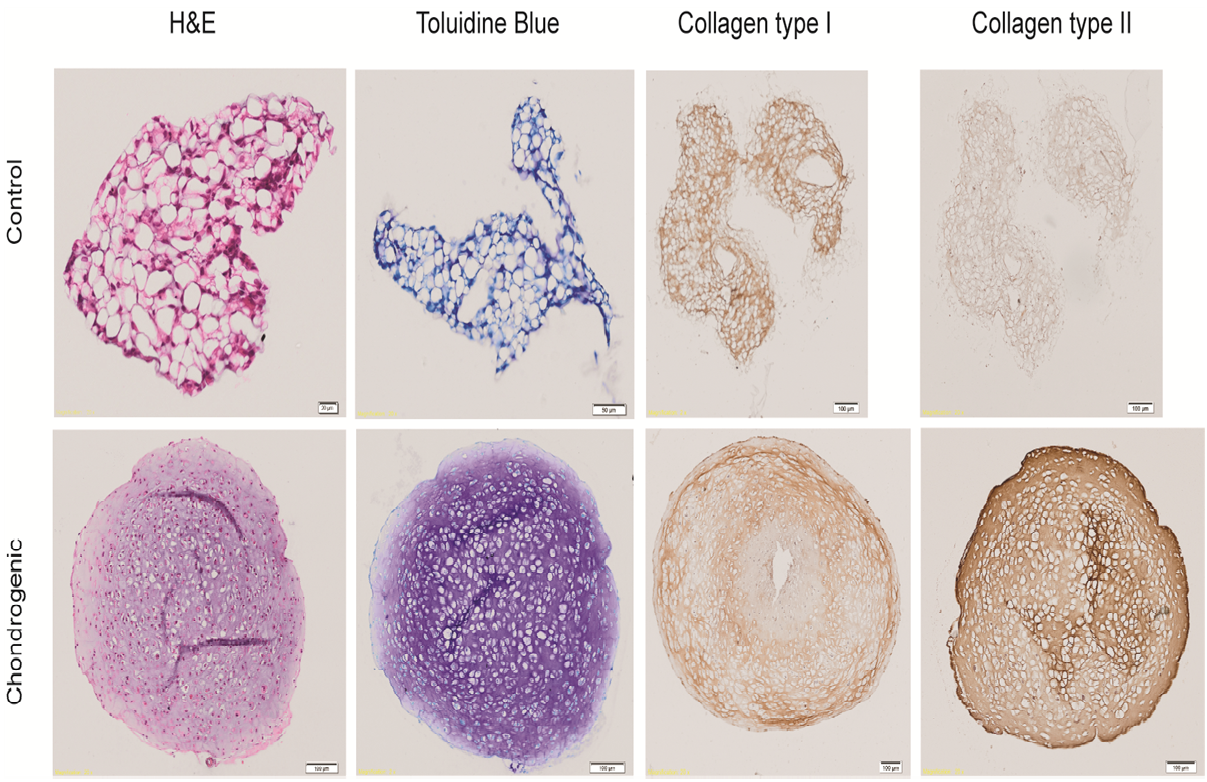

Figure 2 .

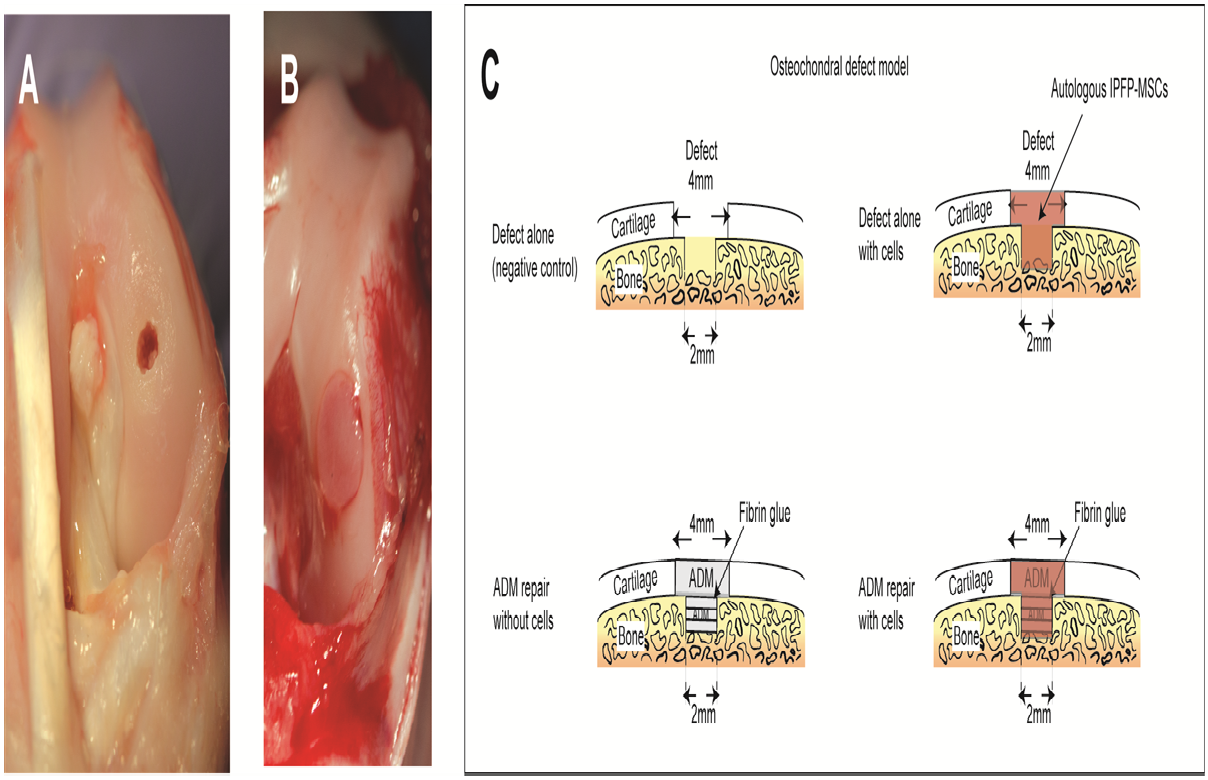

Figure 3 600dpi .

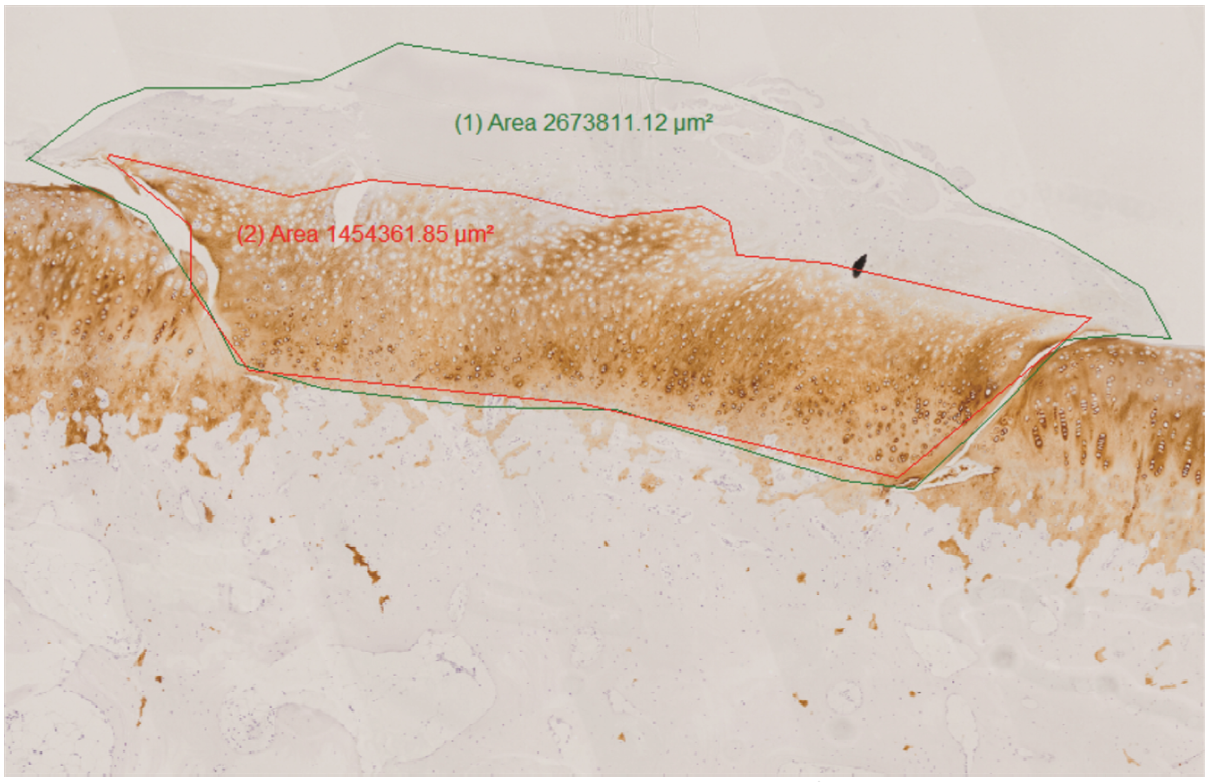

Figure 4 .

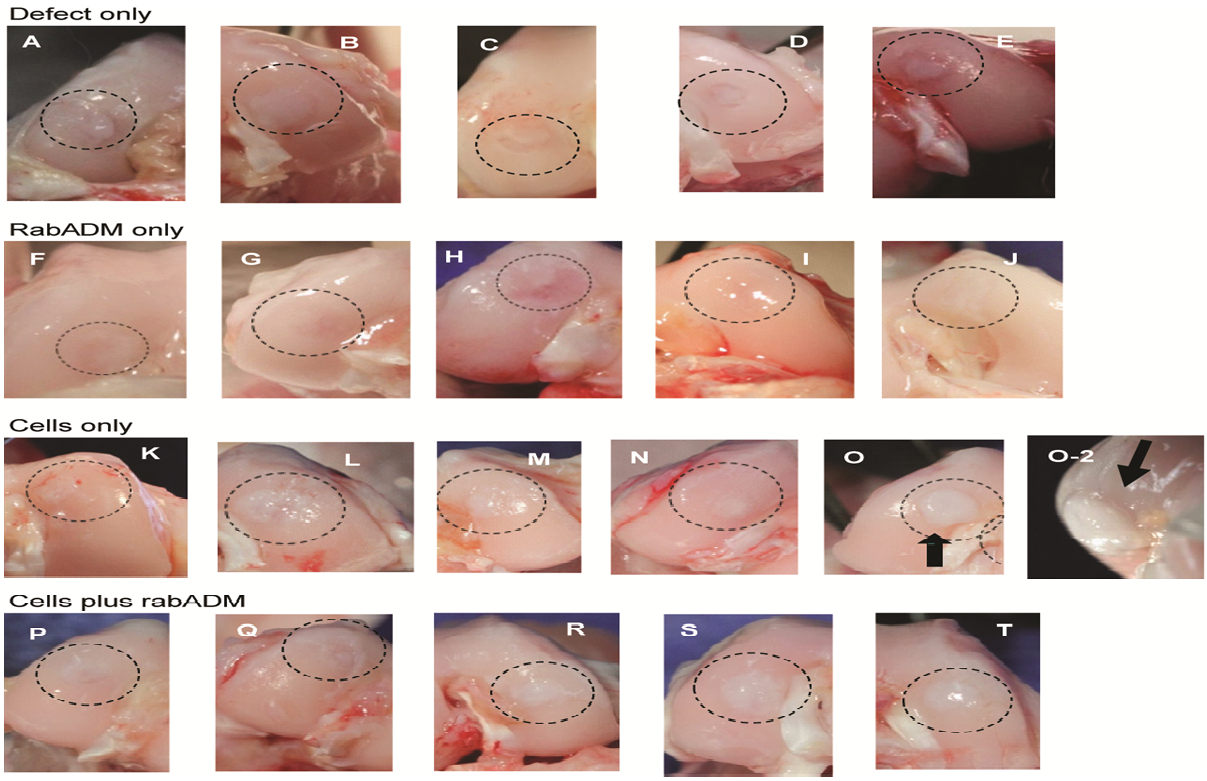

Figure 5 .

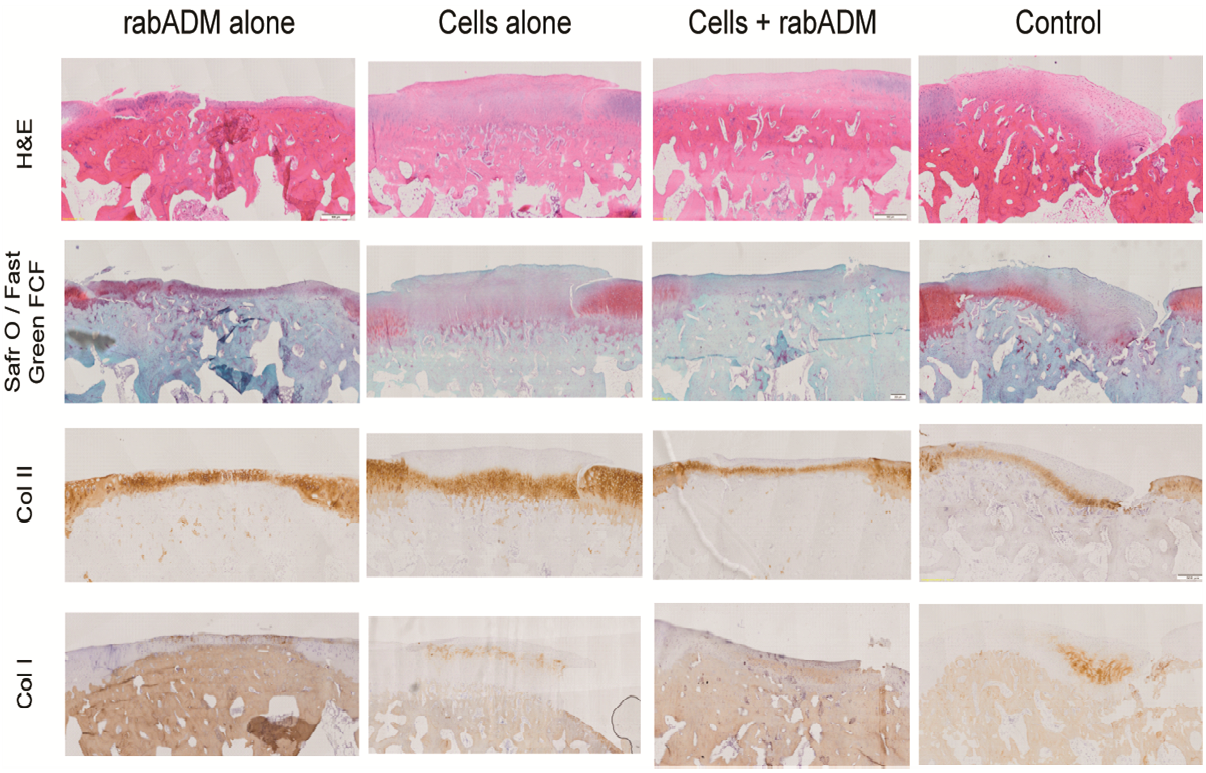

Figure 6 .

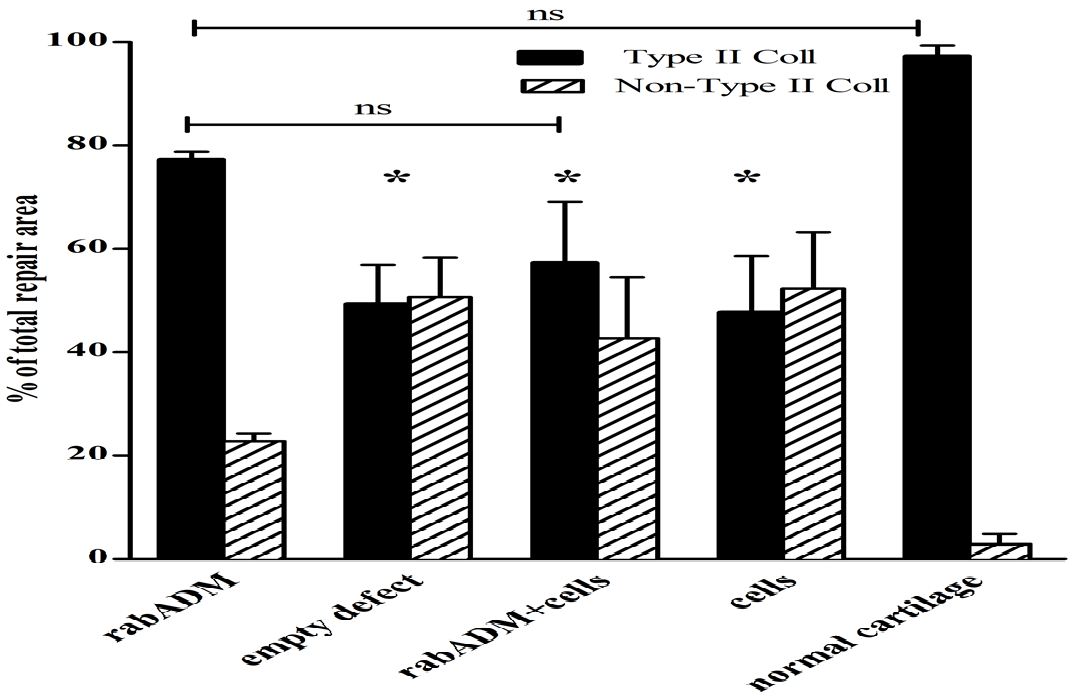

Figure 7 600dpi .